Robust Mouse Pattern Electroretinograms Derived Simultaneously From Each Eye Using a Common Snout Electrode

Tsung-Han Chou,[1] Jorge Bohorquez,[2] Jonathon Toft-Nielsen,[2] Ozcan Ozdamar,[2] and Vittorio Porciatti[1]

[1]Bascom Palmer Eye Institute, University of Miami Miller School of Medicine, Miami, Florida, United States
[2]Department of Biomedical Engineering, University of Miami, Miami, Florida, United States

Correspondence: Vittorio Porciatti, Bascom Palmer Eye Institute, McKnight Vision Research Center, 1638 NW 10th Avenue, Room 507A, Miami, FL 33136, USA; vporciatti@med.miami.edu.

Submitted: January 13, 2014
Accepted: March 11, 2014

Citation: Chou T-H, Bohorquez J, Toft-Nielsen J, Ozdamar O, Porciatti V. Robust mouse pattern electroretinograms derived simultaneously from each eye using a common snout electrode. *Invest Ophthalmol Vis Sci*. 2014;55:2469–2475. DOI:10.1167/iovs.14-13943

Purpose. We recorded pattern electroretinograms (PERGs) simultaneously from each eye in mice using binocular stimulation and a common noncorneal electrode.

Methods. The PERG was derived simultaneously from each eye in 71 ketamine/xylazine anesthetized mice (C57BL/6J, 4 months old) from subcutaneous needles (active, snout; reference, back of the head; ground, root of the tail) in response to contrast-reversal of gratings (0.05 cycles/deg, >95% contrast) generated on two custom-made light-emitting diode (LED) tablets alternating at slight different frequencies (OD, 0.984 Hz; OS, 0.992 Hz). Independent PERG signals from each eye were retrieved using one channel continuous acquisition and phase-locking average (OD, 369 epochs of 492 ms; OS, 372 epochs of 496 ms). The PERG was the average of three consecutive repetitions.

Results. Binocular snout PERGs had high amplitude (mean, 25.3 μV, SD 6.6) and no measurable interocular cross-talk. Responses were reliable (test–retest variability within-session, 14%, SD 7; between sessions, 25%, SD 9; interocular asymmetry within-session, 9%, SD 7; between sessions, 13%, SD 5). Retinal ganglion cells (RGCs) were the main source of the binocular snout PERG, as optic nerve crush in three mice abolished the signal.

Conclusions. The PERG, a sensitive measure of RGC function, is used increasingly in mouse models of glaucoma and optic nerve disease. Compared to current methods, the binocular snout PERG represents a substantial improvement in terms of simplicity and speed. It also overcomes limitations of corneal electrodes that interfere with invasive procedures of the eye and facilitates experiments based on comparison between the responses of the two eyes.

Keywords: retinal ganglion cell, pattern electroretinogram, mouse, bioelectric field, noncorneal electrode

Electrical activity in the retina associated with retinal ganglion cell (RGC) function can be evaluated noninvasively by means of the pattern electroretinogram (PERG) in response to contrast-reversal of patterned visual stimuli.[1–3] The PERG is abolished after optic nerve transection in mammals,[1] including mice,[4–6] that results in RGC loss. Thus, the PERG has been used extensively to probe RGC function in clinical conditions affecting RGCs, such as glaucoma and other optic neuropathies.[7–9] The PERG applications have been used increasingly in mouse models, as the PERG may help to understand how genetic diversity relates to specific differences in RGC function and susceptibility to stress and disease, as well as for monitoring progression of disease and the effect of treatments.[4,10–19] Concurrently, studies have been conducted in mouse models to understand better the biological basis of the PERG signal.[4–6,20,21]

Recently, Chou and Porciatti[21] reported that the bioelectrical field associated with the generation of the PERG signal in the mouse drastically differs from the bioelectrical field associated with the generation of the flash ERG.[22] The PERG bioelectric field is consistent with a dipole model whose axis is predominantly orthogonal to the eye axis, whereas the standard dipole model for the flash ERG (FERG) is coaxial.[22] Consequently, while the FERG signal has its maximum amplitude at the corneal pole, the PERG signal is distributed over the entire anterior part of the head, both eyes and the snout being approximately equipotential. Thus, the PERG potentially can be recorded from the snout in the mouse upon pattern stimulation of either eye. We describe a new method for obtaining robust, independent PERGs from each eye simultaneously using asynchronous binocular stimulation and one-channel acquisition of signals recorded from a subcutaneous needle placed in the snout. Compared to previous methods,[16,23] the present method represents a substantial advancement in terms of simplicity, speed, and reliability. Preliminary results have been presented in abstract form (Chou TH, et al. *IOVS* 2013;54:ARVO E-Abstract 6131).

Methods

Animals and Husbandry

All procedures were performed in compliance with the Association for Research in Vision and Ophthalmology (ARVO)

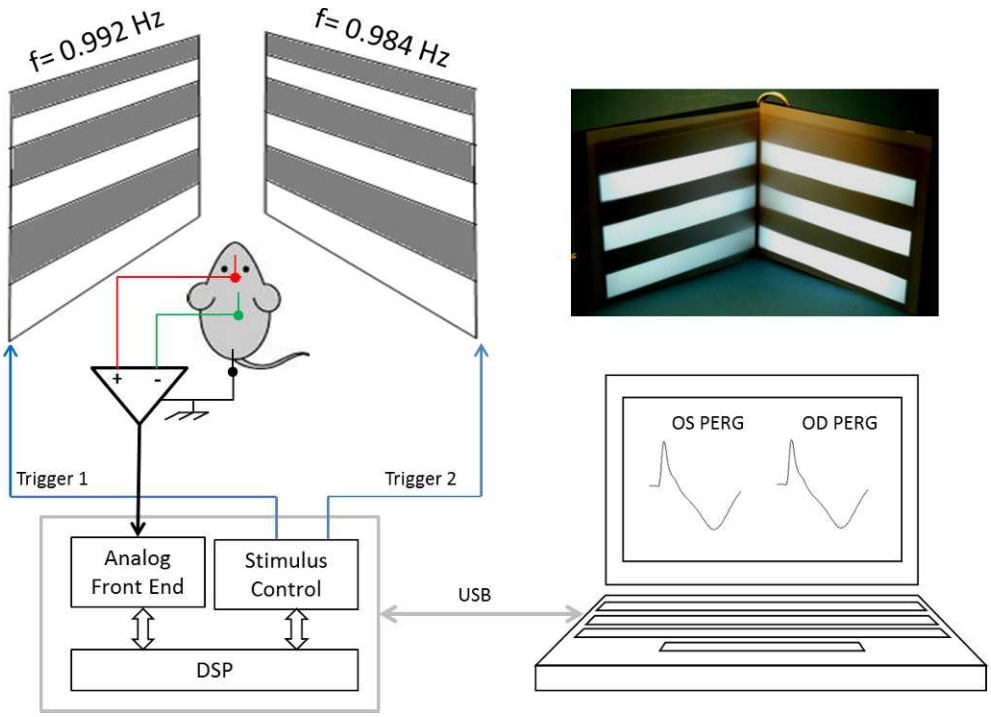

Figure 1. Block diagram for binocular PERG recording. Pattern stimuli are generated on two identical LED displays and presented separately to each eye. The control box generates independent TTL signals to trigger contrast reversal from each display at slightly different frequencies (right eye, 0.984 Hz; left eye, 0.992 Hz. PERG signals are recorded continuously by means of subcutaneous needle electrodes (active, snout; reference, back of the head; ground, tail) and fed to one-channel acquisition system over 183.04 seconds (corresponding to 369 right eye and 372 left eye epochs). The PERG signals for each eye are desynchronized by phase locking averaging method with two noncorrelated frequencies (right eye, every 492 ms; left eye, every 496 ms) and averaged in three consecutive blocks. The grand-average PERG waveforms (approximately 1110 epochs) are displayed on the screen of a laptop that controls the stimulation/acquisition box.

Statement for Use of Animals in Ophthalmic and Vision Research. The experimental protocol was approved by the Animal Care and Use Committee of the University of Miami. A total of 71 mice (C57BL/6J; Jackson Laboratories, Bar Harbor, ME, USA) 4 months old were tested. Mice were maintained in a cyclic light environment (12 hours light, 50 lux–; 12 hours dark) and fed with a grain based diet (Lab Diet, 500, Opti-diet; PMI Nutrition International, Inc., Brentwood, MO, USA).

PERG Recording

Figure 1 shows a diagram of the recording setup. Mice were weighed and anesthetized with intraperitoneal injections (0.5–0.7 mL/kg) of a mixture of ketamine (42.8 mg/mL) and xylazine (8.6 mg/mL). Mice then were restrained gently in a custom-made holder that allowed unobstructed vision. The body of the animal was kept at a constant body temperature of 37.0°C using a rectal probe and feedback-controlled heating pad (TCAT-2LV; Physitemp Instruments, Inc., Clifton, NJ, USA). Pupils were natural and had a diameter smaller than 1 mm[14]; eyes were not refracted for the viewing distance, since the mouse eye has a large depth of focus.[24,25] A small drop of balanced saline was applied topically as necessary to prevent corneal dryness.

The PERG signals were recorded from a subcutaneous stainless steel needle (Grass, West Warwick, RI, USA) placed in the snout. The reference and ground electrodes were similar needles placed medially on the back of the head and at the root of the tail, respectively. Electrical signals were amplified 10,000 times and band-pass filtered (1–300 Hz, 6 dB/oct). We considered the reference electrode as indifferent, as consistent signals cannot not be recorded in response to the pattern stimulus that elicited robust PERGs from either the cornea or snout.[21]

Visual stimuli consisted of contrast-reversing gratings generated on two custom-made tablets (15 × 20 cm) by means of 6 parallel rows of 19 light-emitting diodes (LEDs; LITEON LTW-E670DS, New Taipei City, Taiwan) separated from each other in a framework of alumina-reflective strips and covered with a diffuser. As LEDs emit white light at an angle of 120°, the distance between the LEDs and the diffuser was calculated to have a uniform distribution of light on the surface tablet without perceivable leakage between adjacent rows of LEDs. Using MATLAB software (2011a; MathWorks, Natick, MA, USA), LED rows were switched on and off in counterphase at specific frequencies to generate a pattern of contrast-reversing gratings with an approximately square wave luminance profile (Fig. 1). Detailed description of the LED tablets as well as MATLAB codes for stimulus generation and response analysis is reported in the PhD thesis of Tsung-Han Chou.[26]

At the viewing distance of 10 cm, each stimulus covered an area of 56° vertical × 63° horizontal centered approximately on the projection of the optic disk and was invisible to the contralateral eye. Each stimulus contained 6 horizontal bars (3 white and 3 dark, 0.05 cycles/deg). The mean luminance of the two LED tablets was 500 cd/m^2 as measured by a photometer (OptiCal OP200-E; Cambridge Research Systems Ltd., Rochester, UK). Contrast was >9 %, defined as $C = (Lmax - Lmin)/(Lmax + Lmin)$, where $Lmax$ = luminance of the bright stripes and $Lmin$ = luminance of the dark stripes. A spatial frequency of 0.05 cycles/deg and maximum contrast has been shown previously to elicit PERGs of maximal amplitude.[23] Pattern stimuli were identical for each eye, except that their reversal frequency was slightly different (right eye, 0.992 Hz; left eye,

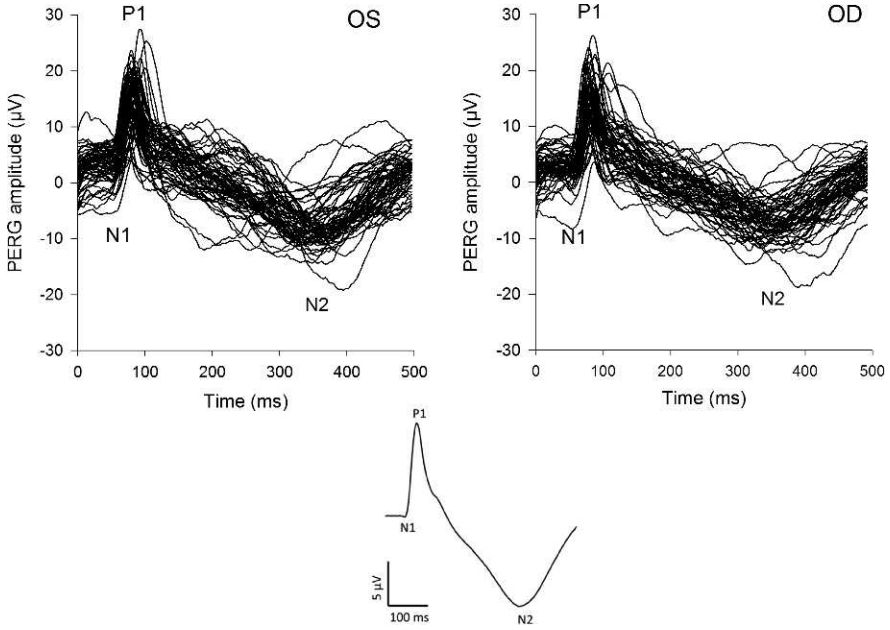

Figure 2. Binocular snout PERGs derived from each eye in response to LED-generated pattern reversal of horizontal gratings in a population of 60 C57BL/6J mice aged 4 months. Individual waveforms of each eye are shown superimposed. Note good reproducibility of PERG waveform across mice, and similarity of responses between the two eyes. The *inset* shows the grand-average of all PERG waveforms from all eyes ($n = 120$). The grand-average PERG waveform is characterized by a small negativity peaking at approximately 50 ms (N1), a major positive wave peaking at approximately 80 ms (P1), and a late negative wave peaking at approximately 350 ms (N2). Response amplitude was calculated from P1 to N2, and response latency as the time-to-peak of P1.

0.984 Hz). A software-controlled digital signal processing (DSP) box (Universal Smart Box; Intelligent Hearing System [IHSYS], Miami, FL, USA) generated transistor-transistor logic (TTL) signals to trigger the circuit of LED pattern reversal with two unsynchronized stimulation rates (right eye, every 492 ms; left eye, every 496 ms). The PERG signal was acquired over 183.024 seconds (corresponding to 369 right eye and 372 left eye epochs) and averaged in synchrony with corresponding TTL triggers. The two stimulation frequencies (0.992 and 0.984 Hz) and the averaging time were calculated to obtain a cancelation of the crosstalk between the responses of the right and left eyes, in agreement with previous published theory that enables cross-talk cancelation in simultaneous recordings of multiple generators.[26,27] The recording protocol was based on three consecutive PERG responses, simultaneously recorded from both eyes. The PERG responses then were superimposed automatically to check for consistency and averaged. The grand-average PERG waveforms were analyzed automatically with MATLAB software (MathWorks) to identify the major positive (P1) and negative waves (N2), and calculate the sum of their absolute values (peak-to-trough amplitude) and the peak latency of the major positive wave (P1).

In four mice (8 eyes) we compared a conventional method (CRT-display/corneal electrodes[11,18,19,23]) with the new LED-display/snout electrode. Patterned stimuli generated on either display were matched for stimulus area (3528°^{2}), spatial frequency (0.05 cycles/deg), and contrast reversal frequency (CRT, 1.0 Hz; LED OD, 0.984 Hz; LED OS, 0.992 Hz), and contrast (>95%), whereas the mean luminance was different (CRT, 50 cd/m^2; LED, 500 cd/m^2). The PERG signals were similarly amplified (×10,000), filtered (1–100 Hz + notch filter), and averaged (CRT, 3 consecutive repetitions of 370 epochs = 1110 epochs; LED OD, 3 consecutive repetitions of 369 epochs = 1107 epochs; LED OS, 3 consecutive repetitions of 372 epochs = 1116 epochs). Due to technical limitations of the CRT setup that did not allow continuous acquisition of the PERG signal, the duration of the waveform displayed was 350 ms, whereas it was 492 ms for the LED OD and 496 ms for the LED OS. This, however, did not impair peak-to-trough amplitude measurement, as the negative trough typically peaked before 350 ms

Results

PERG Waveform

Figure 2 shows a family of binocular snout PERGs derived simultaneously from each eye in response to an LED-generated pattern reversal in a population of 60 C57BL/6J mice aged 4 months. Individual waveforms from each eye are shown superimposed to emphasize common features. Note the similarity of PERG waveforms across different mice, as well as similarity between the two eyes. For the right and left eyes, common features of PERG waveforms consisted of a small negative wave peaking at approximately 50 ms (N1), a positive wave peaking at approximately 80 ms (P1), and a prominent, broad negativity peaking at approximately 350 ms (N2). Note that the waveform onset starts above zero μV on average, as the large negativity is compensated by an upward shift of the entire waveform. The PERG waveform is better visualized in the grand-average of all PERG wave forms from both eyes ($n = 120$). In individual waveforms, response amplitude was calculated from P1 to N2, and response latency as the time-to-peak of P1. The mean PERG P1 to N2 amplitude was OD 25.0 μV, SD 7.2 and OS 25.6 μV, SD 6.1. The mean PERG P1 latency was OD 80.0 ms, SD 6.9 and OS 79.0, SD 6.1. The PERG amplitude and latencies retrieved from the two eyes were not significantly different from each other (latency, $P = 0.2$; amplitude, $P = 0.6$), and were highly correlated, but not identical (amplitude, $R^2 = 0.58$; latency, $R^2 = 0.63$). The approximately 40% residual variance could be explained by

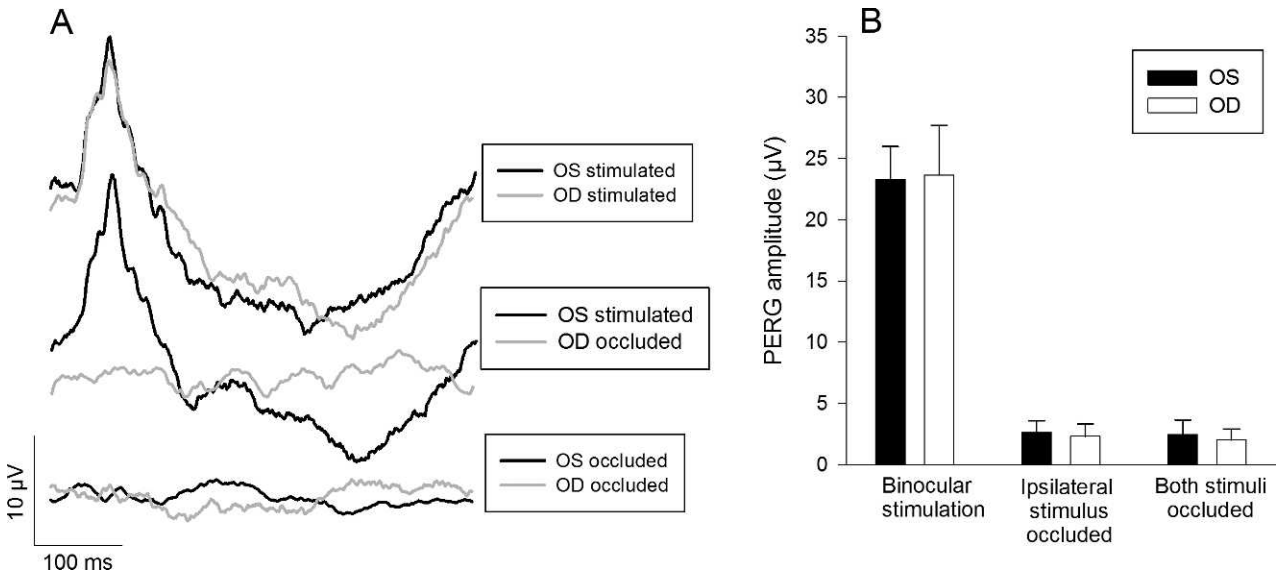

FIGURE 3. Interocular cross-talk is not distinguishable from physiological noise. (**A**) representative example of binocular snout PERGs derived simultaneously from each eye upon binocular stimulation (*upper waveforms*), when one stimulus is occluded (*middle waveforms*), and when both stimuli are occluded (*bottom waveforms*). (**B**) Mean peak-to-trough amplitudes measured in each eye under binocular stimulation, when the stimulus ipsilateral to the recorded eye is occluded, and when both stimuli are occluded. *Error bars* represent the SD ($n = 6$).

interocular differences of PERG signals as well as by the presence of uncorrelated noise which distorted PERG waveforms.

Interocular Cross Talk

As the snout electrode picks up signals generated in both eyes,[21] a first question to ask was whether signals generated in one eye were contaminated by signals generated in the contralateral eye. A straightforward experiment was to occlude one eye and control whether any PERG waveform could be derived from the occluded eye. The representative examples displayed in Figure 3 show that under binocular stimulation PERGs of high amplitude and similar, but not identical, waveform could be derived from each eye; when the right stimulus was occluded, the signal derived from the left eye was virtually unchanged, whereas no identifiable cross-talk signal was derived from the right eye; and the residual signal derived from the eye with occluded stimulus was similar to the physiologic noise, obtained by occluding both eyes. The experiment was repeated in six different mice, resulting in the following peak-to-trough amplitude means: SD ipsilateral stimulus occluded (cross-talk signal) OD 2.3 µV (1.0) and OS 2.6 µV (0.96); both stimuli occluded (physiological noise) OD 2.0 µV (0.91) and OS 2.46 µV (1.16). The amplitude difference between cross-talk signals and corresponding physiological noise was not significant ($P > 0.55$).

Comparison With Conventional Methods

Previous methods of PERG recording in the mouse used conventional corneal electrodes and pattern stimuli generated on CRT displays.[11,18,19,23] To provide a direct comparison between the conventional and the proposed method, we recorded PERGs in four mice (8 eyes) in the same session using a conventional setup (CRT-display/corneal electrodes) and the new LED-display/snout electrode (Fig. 4). Visual stimuli were matched for area, spatial frequency, temporal frequency, and contrast (see methods). Two mice were tested first with the LED and then with the CRT setup, while the inverse sequence was used for the other two mice. With the conventional setup, recording was monocular. In two mice the right eye was tested first and the left eye was tested second, while the inverse sequence was used for the other two mice. With the new method, the two eyes were recorded simultaneously. In Figures 4A and 4B, PERG waveforms recorded from each eye are shown superimposed. While both methods generated approximately similar PERG waveforms and were comparable in the two eyes, there appeared to be differences in the peak-to-trough amplitude, and peak latencies between LED/snout PERGs and CRT/cornea PERGs. On average, LED/snout PERGs tended to have moderately larger amplitude (mean difference, +4.0 µV, SD 5.9; $P = 0.058$), and had a shorter and more consistent peak time of the positive wave (mean difference, –8.0 ms, SD 11.1; $P = 0.027$; Fig. 4C) compared to CRT/cornea PERGs.

Reliability of PERG Signals

To be used as a reliable assessment tool, the binocular snout PERG should produce stable and consistent results. We calculated the variability of PERG signals in the same mice recorded multiple times in the same session (keeping the electrode in place) and between different sessions one week apart. For all measures, variability was expressed as coefficient of variation (CoV = SD/mean %). Within-session variability was calculated as CoV of three consecutive partial averages of approximately 370 epochs each, whose grand-average (approximately 1110 epochs) constituted the actual PERG (see Methods). Between-session variability was calculated as Co-V of four serial PERGs obtained one week apart in 7 different mice. Interocular asymmetry was calculated as CoV of PERGs simultaneously derived from each eye. The Table summarizes within- and between-sessions variability of PERG amplitude, latency, and interocular asymmetry. Within- and between-session variabilities of PERG amplitude and latency were not significantly different between the two eyes. Within-session variability of PERG amplitude was approximately 14%, and was smaller ($P < 0.05$) than that between sessions (approximately 25%). Within-session variability of PERG latency was approx-

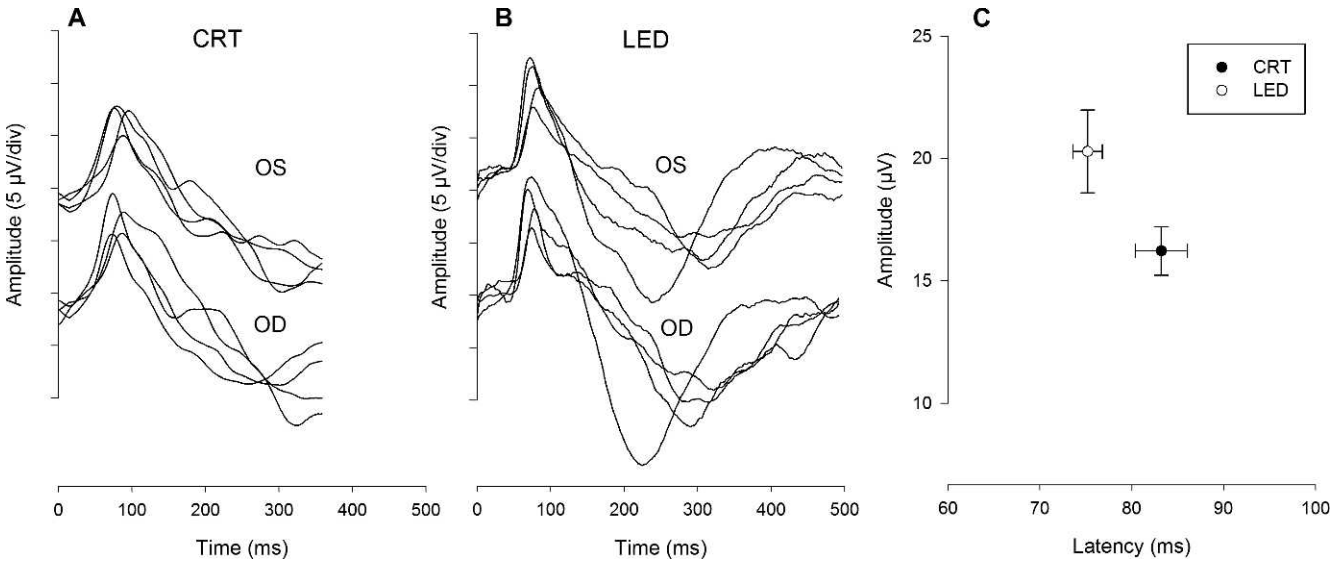

Figure 4. Comparison between corneal and snout PERGs. Responses were recorded in the same mice and session in response to either monocular stimulation using a CRT display and corneal electrodes (**A**) or binocular stimulation using two asynchronous LED displays and one snout electrode (**B**). The CRT and LED stimuli were matched for area, spatial frequency, temporal frequency, contrast, and number of averaged epochs. The luminance of the LED display was higher than that of CRT. (**C**) Comparison of peak-to-trough amplitudes and peak latencies of snout/LED PERGs (*open symbols*) and corneal/CRT PERGs (*filled symbols*). *Bidirectional error bars* represent the SEM ($n = 8$ eyes).

imately 8.5%, and tended to increase between sessions (approximately 11%) although not significantly. Within-session variability of interocular asymmetry for PERG amplitude was approximately 9%, which tended to nonsignificantly increase between-session (approximately 13%). Within-session variability of interocular asymmetry for PERG latency was approximately 4%, and did not change between-sessions.

Validity

As a control that the snout PERG reflected RGC activity as the corneal PERG, we used unpublished data on binocular snout PERG recorded in parallel with corneal PERG from a recent study of Chou et al.[6] In that study, corneal PERGs and photopic FERGs were recorded in 3 C57BL/6J mice before and 1 month after unilateral, intraorbital optic nerve crush (ONC).[6] The RGC counts showed massive (>85%) RGC loss in the operated eyes. Figure 3 of the study of Chou et al.[6] shows that 1 month after ONC, the corneal PERG was dramatically reduced compared to the intact eye together with a major depletion of the RGC population, whereas Figure 4 of that study shows that the FERG was comparable in the two eyes. Figure 5 of the present study shows LED/snout PERGs derived from the right eyes of the 3 mice reported in the study of Chou et al.[6] before and 1 month after ONC. Note that no distinguishable PERG waveforms were recordable in all 3 mice one month after ONC.

Discussion

As the bioelectrical field generated by the PERG signal in the mouse is distributed widely over the entire anterior part of the head,[21] the snout can be used as a common recording site for PERG signals generated in either eye. Our results showed that robust PERG signals from each eye could be retrieved using a subcutaneous needle placed in the snout, asynchronous binocular stimulation, one-channel recording, and a phase locking average method. The PERG signals derived from each eye were independent, as occlusion of one eye generated a signal in the noise range in the same eye, while the signal derived from the contralateral eye was not altered. The PERG signals were robust, the peak-to-trough amplitude being at least as large as that recordable from corneal electrodes using standard CRT displays.[11,16,18,19,23] The signal-to-noise ratio of the binocular snout PERG was of the order of 10, which seems a sufficient dynamic range to monitor PERG changes over severity of disease.

The PERG signals were repeatable within and between sessions, the variability being similar or smaller than that reported for conventional methods with CRT-displays and corneal electrodes.[23] The direct comparison with conventional methods indicated that the present method generates PERG with slightly larger peak-to-trough amplitude, and a shorter and less variable time-to-peak of the P1 wave. These differences may be attributed to several factors, including different location of the recording electrode (the signal recorded from the snout is slightly larger than that recorded from the cornea[21]), the abrupt, spatially synchronous contrast reversal of the LED display compared to the sweeping manner of the CRT-display[28] (asynchrony in activation of contrast detectors can affect the strength of their response as well as smear it in time and delaying the time-to-peak), and the higher mean luminance of the LED display compared to CRT (the PERG is a photopic response that increases in amplitude and shortens in

Table. Summary of Within- and Between-Sessions Variability of PERG Amplitude, Latency, and Interocular Asymmetry

	Within Session		Between Sessions	
	Co-V	SD	Co-V	SD
OS amplitude	14.1	9.1	26.9	11.1
OD amplitude	14.6	5.3	23.1	7.5
OS-OD amplitude asymmetry	9.1	7.1	12.8	5.1
OS latency	6.6	5.4	10.1	5.2
OD latency	10.7	7.4	12.4	5.5
OS-OD latency asymmetry	4.3	5.6	3.9	1.3

For all measures, variability was expressed as CoV = SD/mean %.

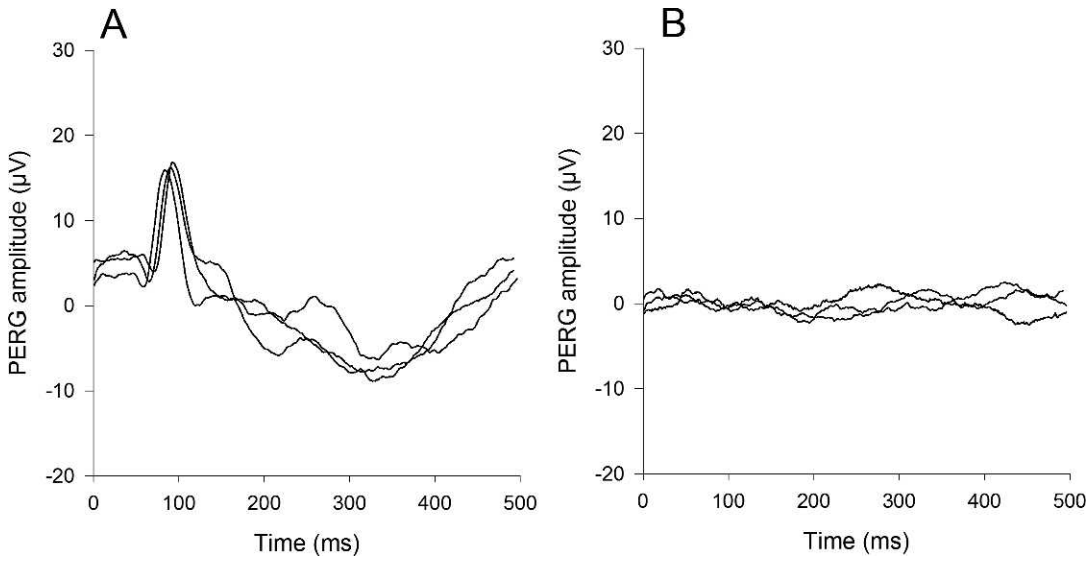

FIGURE 5. Optic nerve crush abolishes the PERG signal. The PERGs were derived from the snout in response to stimulation of the right eye before (**A**) and one month after intraorbital crush of the left optic nerve ([**B**], supplementary results reprinted with permission from study of Chou et al.[6]).

latency with increasing luminance, for example as shown in the study of Porciatti et al.[29]). The use of an LED display was necessary to trigger reversal rates at specific frequencies differing by a fraction of Hz for phase-locking average, as LEDs do not have the constraints of fixed refresh rates of conventional CRT displays. The LED technology also allowed us to design small, lightweight displays that could be presented simultaneously and independently to each eye from close distance without substantial electromagnetic interference pick up from the recording electrode typical of CRT displays.

The LED-generated binocular PERGs from the snout have a number of practical advantages compared to standard monocular PERGs from corneal electrodes. The first obvious advantages are simplicity and speed, as electrode placement is effortless; thus, minimizing operator-dependent time and variability, and the recording time is halved. The second advantage is that the PERG signal is at least as robust and reliable as conventional CRT-generated PERG. A third, important advantage is that simultaneous recording from each eye using a common noncorneal electrode minimizes interocular differences originating from electrode-related variables as well as time-related variables, such as depth of anesthesia. This greatly facilitates experiments in which one eye is used as test and the other used as control. It also overcomes limitations of corneal electrodes that interfere with invasive procedures, such as intraocular injections and optic nerve surgery. Finally, the use of a subcutaneous electrode greatly facilitates recording under challenging conditions, such as body inversion to induce elevation of the intraocular pressure.[13,14]

In conclusion, the binocular snout PERG appears to be a solid method for high throughput assessment of RGC function in mouse models of RGC injury, including glaucoma and other optic nerve neuropathies, phenotypic screening of genotypically diverse mouse strains and for studies of toxicity and drug testing.

Acknowledgments

Supported by National Institutes of Health (NIH) Grant NIH-NEI RO1 EY019077, NIH center Grant P30-EY014801, and an unrestricted grant to Bascom Palmer Eye Institute from Research to Prevent Blindness, Inc.

Disclosure: **T.-H. Chou**, None; **J. Bohorquez**, None; **J. Toft-Nielsen**, None; **O. Ozdamar**, None; **V. Porciatti**, None

References

1. Maffei L, Fiorentini A. Electroretinographic responses to alternating gratings before and after section of the optic nerve. *Science*. 1981;211:953–955.
2. Sieving PA, Steinberg RH. Proximal retinal contribution to the intraretinal 8-Hz pattern ERG of cat. *J Neurophysiol*. 1987;57:104–120.
3. Zrenner E. The physiological basis of the pattern electroretinogram. In: Osborne N, Chader G, eds. *Progress in Retinal Research*. Oxford, UK: Pergamon Press; 1990:427–464.
4. Porciatti V, Pizzorusso T, Cenni MC, Maffei L. The visual response of retinal ganglion cells is not altered by optic nerve transection in transgenic mice overexpressing Bcl-2. *Proc Natl Acad Sci U S A*. 1996;93:14955–14959.
5. Miura G, Wang MH, Ivers KM, Frishman LJ. Retinal pathway origins of the pattern ERG of the mouse. *Exp Eye Res*. 2009;89:49–62.
6. Chou TH, Park KK, Luo X, Porciatti V. Retrograde signaling in the optic nerve is necessary for electrical responsiveness of retinal ganglion cells. *Invest Ophthalmol Vis Sci*. 2013;54:1236–1243.
7. Bach M, Brigell MG, Hawlina M, et al. ISCEV standard for clinical pattern electroretinography (PERG): 2012 update. *Doc Ophthalmol*. 2013;126:1–7.
8. Ventura LM, Porciatti V. Pattern electroretinogram in glaucoma. *Curr Opin Ophthalmol*. 2006;17:196–202.
9. Holder GE. Pattern electroretinography (PERG) and an integrated approach to visual pathway diagnosis. *Prog Retin Eye Res*. 2001;20:531–561.
10. Rossi FM, Pizzorusso T, Porciatti V, Marubio LM, Maffei L, Changeux JP. Requirement of the nicotinic acetylcholine receptor beta 2 subunit for the anatomical and functional development of the visual system. *Proc Natl Acad Sci U S A*. 2001;98:6453–6458.
11. Howell GR, Libby RT, Jakobs TC, et al. Axons of retinal ganglion cells are insulted in the optic nerve early in DBA/2J glaucoma. *J Cell Biol*. 2007;179:1523–1537.

Investigative Ophthalmology & Visual Science

12. Saleh M, Nagaraju M, Porciatti V. Longitudinal evaluation of retinal ganglion cell function and IOP in the DBA/2J mouse model of glaucoma. *Invest Ophthalmol Vis Sci*. 2007;48:4564–4572.
13. Porciatti V, Nagaraju M. Head-up tilt lowers IOP and improves RGC dysfunction in glaucomatous DBA/2J mice. *Exp Eye Res*. 2010;90:452–460.
14. Nagaraju M, Saleh M, Porciatti V. IOP-dependent retinal ganglion cell dysfunction in glaucomatous DBA/2J mice. *Invest Ophthalmol Vis Sci*. 2007;48:4573–4579.
15. Enriquez-Algeciras M, Ding D, Chou TH, et al. Evaluation of a transgenic mouse model of multiple sclerosis with noninvasive methods. *Invest Ophthalmol Vis Sci*. 2011;52:2405–2411.
16. Porciatti V, Chou TH, Feuer WJ. C57BL/6J, DBA/2J, and DBA/2J.Gpnmb mice have different visual signal processing in the inner retina. *Mol Vis*. 2010;16:2939–2947.
17. Howell GR, Soto I, Zhu X, et al. Radiation treatment inhibits monocyte entry into the optic nerve head and prevents neuronal damage in a mouse model of glaucoma. *J Clin Invest*. 2012;122:1246–1261.
18. Enriquez-Algeciras M, Ding D, Mastronardi FG, Marc RE, Porciatti V, Bhattacharya SK. Deimination restores inner retinal visual function in murine demyelinating disease. *J Clin Invest*. 2013;123:646–656.
19. Yu H, Koilkonda RD, Chou TH, et al. Gene delivery to mitochondria by targeting modified adenoassociated virus suppresses Leber's hereditary optic neuropathy in a mouse model. *Proc Natl Acad Sci U S A*. 2012;109:E1238–E1247.
20. Yang X, Chou T-H, Ruggeri M, Porciatti VA. New mouse model of inducible, chronic retinal ganglion cell dysfunction not associated with cell death. *Invest Ophthalmol Vis Sci*. 2013;54:1898–1904.
21. Chou TH, Porciatti V. The bioelectric field of the pattern electroretinogram in the mouse. *Invest Ophthalmol Vis Sci*. 2012;53:8086–8092.
22. Rodieck RW. Components of the electroretinogram–a reappraisal. *Vision Res*. 1972;12:773–780.
23. Porciatti V, Saleh M, Nagaraju M. The pattern electroretinogram as a tool to monitor progressive retinal ganglion cell dysfunction in the DBA/2J mouse model of glaucoma. *Invest Ophthalmol Vis Sci*. 2007;48:745–751.
24. Remtulla S, Hallett PE. A schematic eye for the mouse, and comparisons with the rat. *Vision Res*. 1985;25:21–31.
25. Schmucker C, Schaeffel F. A paraxial schematic eye model for the growing C57BL/6 mouse. *Vision Res*. 2004;44:1857–1867.
26. Chou T-H. *Age-Related Structural and Functional Changes of the Mouse Eye: Role of Intraocular Pressure and Genotype. Biomedical Engineering*. Miami, FL: University of Miami Scholarly Repository; 2011:94.
27. Ozdamar O, Bohorquez J. Asynchronized multi-stimulus averaging deconvolution (AMAD) of auditory evoked potentials. In: *XXIII Meeting of the International Evoked Response Audiometry Study Group (IERASG)*. New Orleans, LA: IERAG; 2013:46.
28. Toft-Nielsen J, Bohorquez J, Ozdamar O. Innovative pattern reversal displays for visual electrophysiological studies. *Conf Proc IEEE Eng Med Biol Soc*. 2011;2011:2009–2012.
29. Porciatti V, Burr DC, Morrone MC, Fiorentini A. The effects of aging on the pattern electroretinogram and visual evoked potential in humans. *Vision Res*. 1992;32:1199–1209.

Investigative Ophthalmology & Visual Science